Met. Mater. Int., Vol. 23, No. 2 (2017), pp. 308~312
doi: 10.1007/s12540-017-6564-5

Effect of Aging Time and Temperature on the Aging Behavior in Sn Containing AZ91 Alloy

Jeong Kyun Kim[1], Seung Hyun Oh[1], Kang Cheol Kim[1], Won Tae Kim[2], and Do Hyang Kim[1,*]

[1]Department of Metallurgical Engineering, Center for Noncrystalline Materials, Yonsei University, Seoul 03722, Republic of Korea
[2]Department of Optical Engineering, Cheongju University, Cheongju 28503, Republic of Korea

(received date: 12 August 2016 / accepted date: 12 September 2016)

Effects of aging temperature and time on the aging behavior in AZ91 alloy and Sn containing AZ91 alloy (AZT915) have been investigated in the present study. The mode of precipitation, i.e. discontinuous and continuous precipitation in both alloys is strongly affected by the aging temperature. At low aging temperature of 403 K, only discontinuous precipitation occurs at the grain boundaries, whereas at high aging temperatures of 573 and 623 K only continuous precipitation occurs inside the grains. At intermediate temperature range (443 or 498 K) both discontinuous and continuous precipitation reactions occur. In AZT915, the Mg_2Sn particles at the grain boundary effectively reduce the available nucleation sites for discontinuous β precipitates, and slow down the movement of the grain boundary, resulting in suppression of discontinuous precipitation. In addition, increased local lattice strain by the presence of Sn in the α-Mg solid solution matrix accelerates the nucleation of the continuous precipitates at the early stage of aging treatment. Therefore, significantly higher peak hardness can be obtained within a shorter aging time in AZT915.

Keywords: aging, precipitation, hardness test, AZ91D, Mg-Al-Zn-Sn

1. INTRODUCTION

Magnesium alloys have a great potential as attractive light weight alloys particularly for the automotive industry due to their low density and high specific strength. Among the commercial magnesium alloys, Mg-Al based alloys are known to exhibit the best combination of castability, resistance to corrosion and mechanical properties [1-5]. According to the equilibrium phase diagram, the maximum solid solubility of aluminum in magnesium is ~2 wt% at room temperature and increases up to ~12.7 wt% at 710 K [6], which enables strengthening by precipitation. In fact, the mechanical property of AZ91 (Mg-9Al-0.8Zn-0.3Mn, in wt%) alloy can be improved by precipitation of $Mg_{17}Al_{12}$ (β) in the α-Mg matrix [7]. It is well known that two types of precipitates form in aged AZ91 alloy, i.e. discontinuous and continuous precipitates. The discontinuous precipitation occurs by cellular growth of alternating plates of the β secondary phase and the α-Mg matrix phase at grain boundaries [8]. Such a heterogeneous reaction can be activated by the simultaneous effects from formation of lamellar structure of alternating two phases and movement of grain boundaries at the aging temperature. On the other hand, continuous precipitation occurs by forming long lath-shaped plates inside the α-Mg grains. These continuous precipitates have an orientation relationship with the matrix [9]. The age hardening response is influenced by the density, size and shape of β precipitates [10,11].

Since the discontinuous precipitation is known to deteriorate the strengthening effect, many studies have been performed to suppress the discontinuous precipitation during aging treatment of AZ91 alloy. It has been reported that addition of Pb, Ca and RE (rare earth element) suppresses the discontinuous precipitation [12,13]. Recently, it has been shown that addition of Sn in AZ91 alloy not only suppresses the discontinuous precipitation at grain boundary but also accelerates the continuous precipitation inside the grain, significantly enhancing the age hardening response [14]. Although Sn is known to be effective in changing the precipitation mode in AZ91 alloy, the effects of aging temperature and time have not been reported in detail yet. Therefore, the aim of the present study is to investigate the effect of aging time and temperature on the precipitation behavior of 5 wt% Sn containing AZ91 alloy. For comparison, precipitation and age hardening behavior of AZ 91 alloy is investigated.

2. EXPERIMENTAL PROCEDURE

AZ91 (Mg-9Al-0.8Zn-0.3Mn) and 5 wt% Sn-added AZ91

*Corresponding author: dohkim@yonsei.ac.kr

(Mg-9Al-0.8Zn-0.3Mn-5Sn) alloys (will be referred to as AZ91, AZT915) were prepared by melting a minimum purity of 99.9 wt% metallic elements under a protective mixture of SF_6 and CO_2 atmosphere at 1023 K and then pouring into a preheated rectangular steel mold with a dimension of 10 mm in thickness, 60 mm in width, and 100 mm in height. Solution solid treatment was conducted at 683 K for 24 h, and then the samples were immediately water-quenched. Solution-treated specimens were aged at 423 K, 443 K, 498 K, 573 K and 623 K for different times up to 24 h. Age hardening response was investigated by using Vickers hardness measurements (MXT-ZX7E) under a load of 1 kg_f. Microstructure of the specimens etched with a nital solution was observed by scanning electron microscopy (SEM, JSM7001F). Specimens for transmission electron microscopy (TEM, JEM2000EX) were prepared using an ion milling equipment (Gatan™, model 600).

3. RESULTS

Figure 1 shows the SEM images obtained from AZ91 and AZT915 aged at 423 K for 1 and 8 h. In the case of AZ91, discontinuous precipitates began to appear at grain boundary after aging for 1 h (Fig. 1(a)), and grew extensively after aging for 8 h (Fig. 1(c)). In the case of AZT915, discontinuous precipitates began to appear after aging for 1 h (Fig. 1(b)). Mg_2Sn particles were present at the grain boundaries due to addition of Sn. Mg_2Sn particles remained at the grain boundaries after solution treatment due to its high melting temperature of ~1043 K [15]. The most striking difference between AZ91 and AZT915 was that discontinuous precipitation was almost completely suppressed by the addition of Sn in AZ91, as evidenced from the micrograph obtained after aging for 8 h (Fig. 1(d)).

Figure 2 show SEM images obtained from AZ91 and AZT915 after aging for 4 h at the different temperatures of 443 K, 498 K, 573 K and 623 K. At the aging temperature of 443 K, discontinuous precipitates grew extensively, but continuous precipitation did not occur inside the α-Mg grains in AZ91 (Fig. 2(a)). In the case of AZT915, discontinuous precipitation was almost completely suppressed at the grain boundaries, but fine continuous precipitates were observed inside the α-Mg grains (Fig. 2(b)). To clarify the early stage precipitation behavior, the samples aged for 1 h at 443 K were observed by TEM (Fig. 3). Very few precipitates were observed in AZ91 (Fig. 3(a)), whereas fine continuous precipitates with a high density were observed in AZT915 (Fig. 3(b)). The result in Fig. 3 implies that the continuous precipitation is highly accelerated even at early stage of precipitation by addition of Sn in AZ91. When the aging temperature was raised up to 498 K, highly dense continuous precipitates appeared inside the α-Mg grains in AZ91 (Fig. 2(c)) as well as in AZT915 (Fig. 2(d)). Only the difference was that large portion of discontinuous precipitates were presented at the grain boundaries

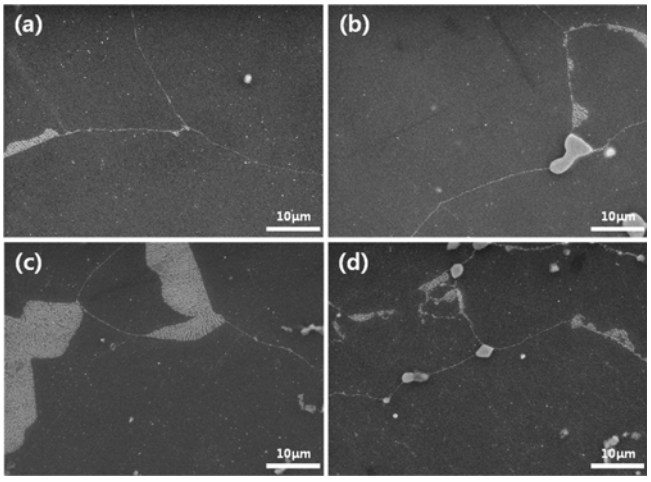

Fig. 1. Secondary electron micrographs of: (a) AZ91 and (b) AZT915 after aging at 423 K for 1 h; and (c) AZ91 and (d) AZT915 after aging at 423 K for 8 h.

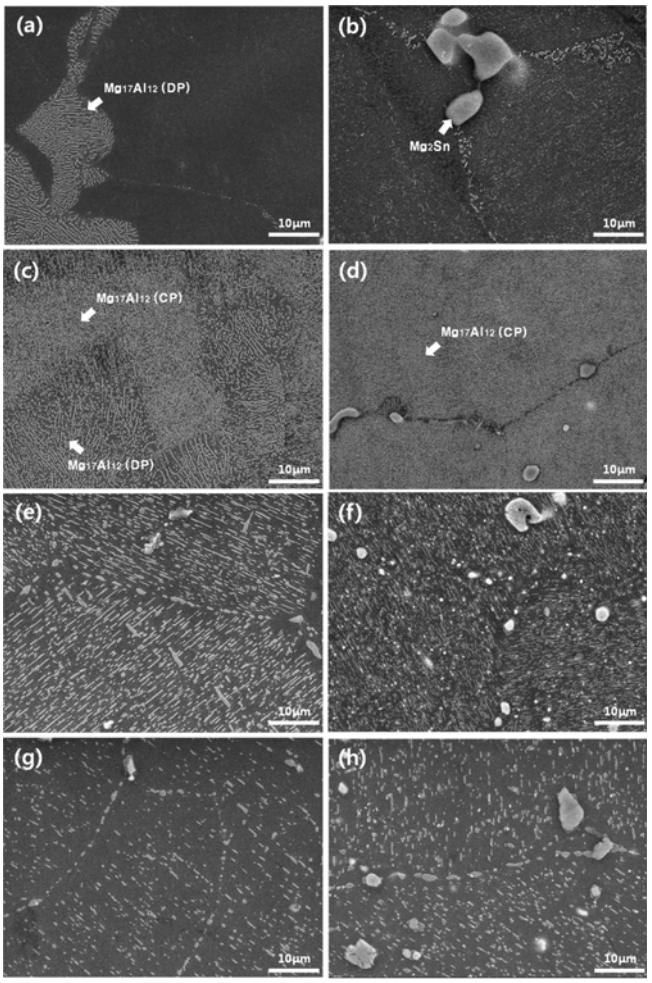

Fig. 2. Secondary electron micrographs of: (a) AZ91 and (b) AZT915 after aging at 443 K for 4 h; (c) AZ91 and (d) AZT915 after aging at 498 K for 4 h; (e) AZ91 and (f) AZT915 after aging at 573 K for 4 h; and (g) AZ91 and (h) AZT915 after aging at 623 K for 4 h.

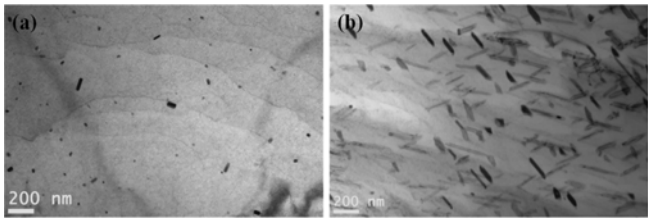

Fig. 3. Bright TEM images obtained from: (a) AZ91 and (b) AZT915 after aging at 443 K for 1 h.

of AZ91, while very small fraction of discontinuous precipitates were presented at the grain boundaries of AZT915. When the aging temperature was increased to 573 K, discontinuous precipitates were not observed in both of AZ91 and AZT915 (Figs. 2(e) and (f)). Instead, only continuous precipitates were observed in both alloys. Only the difference was that finer continuous precipitates with a higher density were formed in the α-Mg matrix of AZT915. At the aging temperature of 623 K, only continuous precipitation occurred in AZ91 (Fig. 2(g)) as well as in AZT915 (Fig. 2(h)). However, the density of the precipitates decreased significantly, when compared to the samples aged at 573 K (Figs. 2(e) and (f)) due to high aging temperature closed to solvus temperature.

The schematics in Fig. 4 summarize the microstructural evolution due to precipitation in AZ91 and AZT915 depending on aging temperature and time. Based on the result in Fig. 4, time-temperature-precipitation (TTP) diagram is introduced in Fig. 5. The TTP diagram indicates that the mode of precipitation, i.e. discontinuous and continuous precipitation in AZ91 and AZT915 is strongly affected by the aging temperature. At low aging temperature of 403 K, only discontinuous precipitation occurs at the grain boundaries, whereas at high aging temperatures of 573 and 623 K only continuous precipitation occurs inside the grains. The TTP diagram also indicates that at intermediate temperature range (443 or 498 K) both discontinuous and continuous precipitation reactions occur. Here, the most

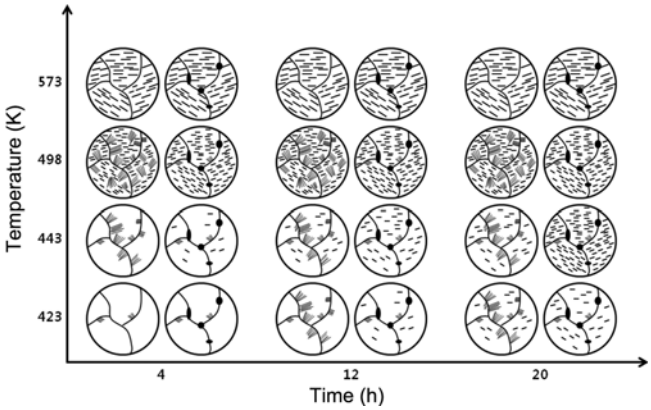

Fig. 4. The schematics showing the microstructural evolution in AZ91 and AZT915, depending on aging temperature and time.

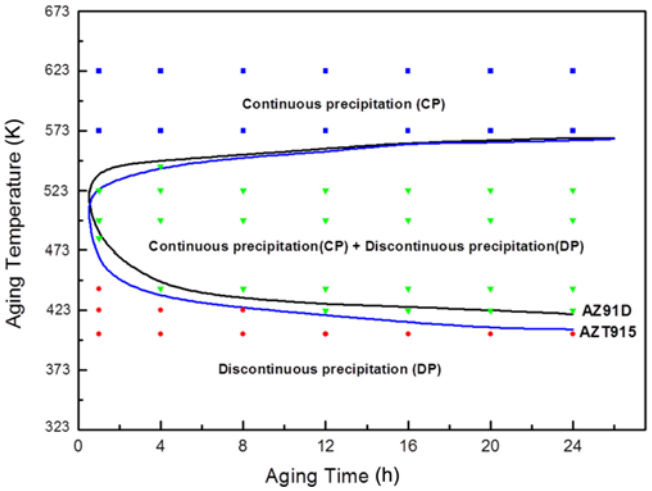

Fig. 5. Time-temperature-precipitation diagram for AZ91 and AZT915 alloys.

noticeable features of AZT915 at the intermediate aging temperature range are: 1) the continuous precipitates start to form much earlier than AZ91; and 2) the fraction of discontinuous precipitates in the continuous + discontinuous precipitation region is significantly decreased. In general, continuous precipitation tends to be favored at high temperatures of aging, whereas at low temperatures of aging, discontinuous precipitation is favored.

Figures 6(a) and (b) show the variation of hardness of AZ91 and AZT915, respectively, depending on aging temperature and time. The hardness was measured at the aging temperatures of 423, 443, 498, 523, 573 and 623 K up to 24 h. The result clearly shows that the overall hardness increase during aging treatment becomes significantly higher with the addition of Sn. Maximum hardness value in AZ91 at each aging temperature was 72 H_V (at 423 K for 20 h), 80 H_V (at 443 K for 16 h, highest hardness value in AZ91), 77 H_V (at 498 K for 8 h), and 76 H_V (at 523 K for 4 h). Any discernible hardness increase was not observed when the aging temperature was 573 K and 623 K. Maximum hardness value in AZT915 at each aging temperature was 84 H_V (at 423 K for 16 h), 92 H_V (at 443 K for 12 h, highest hardness value in AZT915), 86 H_V (at 498 K for 4 h) and 84 H_V (at 523 K for 4 h). As in AZ91, any discernible hardness increase was not observed when the aging temperature was 573 K and 623 K. Here, it can be noticed that hardening response at the early stage of aging process is significantly enhanced in Sn containing AZ91 alloy. For example, in the case of aging at 443 K, the hardness value in AZ91 increases: 54 Hv (after solution treatment), 57 Hv (1 h) - 66 Hv (4 h) - 75 Hv (8 h) - 77 Hv (12 h) - 80 Hv (16 h, peak aged condition), while in AZT915, 62 Hv (after solution treatment) - 68 Hv (1 h) - 78 Hv (4 h) - 88 Hv (8 h) - 92 Hv (12 h, peak aged condition), indicating that the aging time required for peak aged condition is decreased, and simultaneously the hardness level at peak aged condition is increased,

due to superior hardening response at the early stage of aging treatment in Sn containing AZ91 alloy.

4. DISCUSSION

The present study shows that continuous and/or discontinuous precipitation reactions occur depending on the aging temperature in AZ91 and AZT915. Both continuous and discontinuous precipitation reactions are typical examples of solid-state diffusional phase transformation, however, the difference between them originates from the nucleation and growth mechanism. The discontinuous precipitation occurs by the growth of alternating β and α-Mg layers behind a moving grain boundary, whereas the continuous precipitation proceeds by nucleation and growth of β precipitates inside the α-Mg grains. The TTP diagram in Fig. 5 indicates that discontinuous precipitation is preferred at lower temperature of aging (423 K), but continuous precipitation is preferred at higher aging temperature (573 K and 623 K), which is in agreement with the previous report [16]. Since grain boundary diffusion is more activated than volume diffusion at lower temperature [17], discontinuous precipitates begin to form at the grain boundaries during aging process at lower temperature. As the aging temperature increases, volume diffusion becomes faster, thus continuous precipitation initiates inside the α-Mg grains. If continuous precipitates begin to form inside the grains, then discontinuous precipitation is stopped. At higher aging temperature near solvus temperature, volume diffusion dominates the diffusion mechanism, resulting in occurrence of only continuous precipitation inside the α-Mg grains.

Although the TTP curves obtained from AZ91 and AZT915 are similar in shape, there are two main differences: almost complete suppression of discontinuous precipitation and highly activated continuous precipitation at early stage of aging in AZT915. The tendency for discontinuous precipitation is basically dependent on various factors such as nucleation rate of β at the grain boundaries, grain boundary movement velocity, interlamellar spacing, temperature, solute content and conditions of the grain boundaries [16]. In Sn containing AZ91 alloy, the Mg_2Sn particles at the grain boundary effectively reduce the available nucleation sites for discontinuous β precipitates, and slow down the movement of the grain boundary, resulting in suppression of discontinuous precipitation. On the other hand, the tendency for continuous precipitation is determined by the number of available nucleation sites for continuous precipitates. Therefore, the amount of continuous precipitates is strongly dependent on the number of heterogeneous nucleation sites, i.e. the number of crystal defects inside the grains. Therefore, the acceleration of the nucleation rate of the continuous precipitates at the early stage of aging treatment in AZT915 is considered to be due to increase of local lattice strain by the presence of Sn in the α-Mg solid solution matrix.

The result of hardness measurement in Fig. 6 shows that

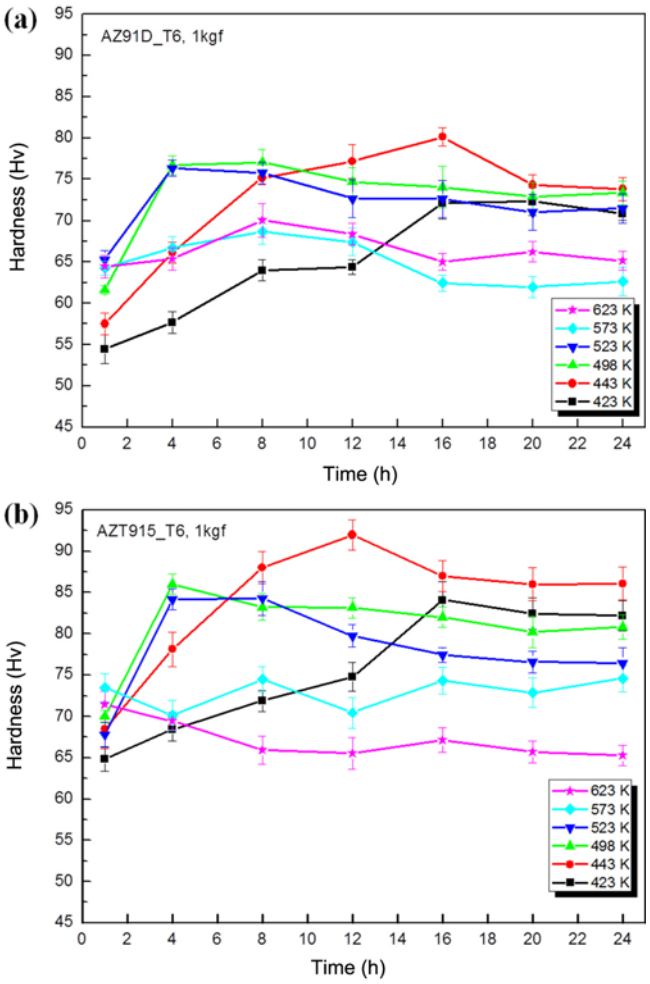

Fig. 6. Variation of Vickers hardness value during aging treatment of: (a) AZ91 and (b) AZT915.

the addition of Sn is very effective in enhancing the aging response in AZ91, thus in obtaining higher hardness value. It should be pointed out that: 1) the hardness after solid solution treatment in AZT915 is higher than in AZ91 (due to particle strengthening effect by Mg_2Sn particles at the grain boundaries and solid solution strengthening effect by the Sn solute in the matrix); and 2) the hardness increases more steeply with the start of the aging treatment (due to suppression of discontinuous precipitation and acceleration of continuous precipitation). Therefore, significantly higher peak hardness can be obtained within a shorter aging time in Sn containing alloy. However, the results in the previous studies show that the effect of minor alloying elements on the age hardening behavior has not been consistent, i.e. it has been shown that the addition of Pb, Ca, Au and RE elements delays the hardening kinetics or decreases the peak hardness value, in spite of suppression of discontinuous precipitation [12,18,19]. Considering from the result in the present study, the addition of Pb, Ca, Au and RE elements may have little contribution on

the activation of continuous precipitation inside the grains, resulting in deteriorated aging response.

5. CONCLUSION

Effects of aging temperature and time on the aging behavior in Sn containing AZ91 alloy have been investigated in the present study. The main conclusions are as follows:

(1) The mode of precipitation, i.e. discontinuous and continuous precipitation in AZ91 and AZT915 is strongly affected by the aging temperature. At low aging temperature of 403 K, only discontinuous precipitation occurs at the grain boundaries, whereas at high aging temperatures of 573 and 623 K only continuous precipitation occurs inside the grains. At intermediate temperature range (443 or 498 K) both discontinuous and continuous precipitation reactions occur.

(2) In Sn containing AZ91 alloy, the Mg_2Sn particles at the grain boundary effectively reduce the available nucleation sites for discontinuous β precipitates, and slow down the movement of the grain boundary, resulting in suppression of discontinuous precipitation. In addition, increased local lattice strain by the presence of Sn in the α-Mg solid solution matrix accelerates the nucleation of the continuous precipitates at the early stage of aging treatment.

(3) In Sn containing AZ91 alloy, significantly higher peak hardness can be obtained within a shorter aging time due to higher hardness after solution treatment - water quenching and more steeply increase of hardness with the start of aging treatment.

ACKNOWLEDGEMENT

This study was supported by the Important Defense Materials Technology Development project funded by the Korea Ministry of Industrial, Trade and Energy.

REFERENCES

1. D. Wenwen, S. Yangshan, and W. Dengym, *Mat. Sci. Eng. A* **356**, 1 (2003).
2. J. H. Jun and J. H. Moon, *Met. Mater. Int.* **21**, 780 (2015).
3. Y. I. Choi, K. Kuroda, and M. Okido, *Met. Mater. Int.* **21**, 857 (2015).
4. H.-T. Son, Y.-H. Kim, J.-H. Kim, H.-S. Yoo, and J.-W. Choi, *Korean J. Met. Mater.* **53**, 336 (2015).
5. S. Y. Park, S. K. Kim, and D. B. Lee, *Korean J. Met. Mater.* **54**, 390 (2016).
6. A. Srinivasan, U. T. S. Pillai, and B. C. Pai, *Mat. Sci. Eng. A* **452–453**, 87 (2007).
7. J. B. Clark, *Acta Metall. Mater.* **16**, 141 (1968).
8. D. B. Willams and F. P. Butler, *Int. Met. Rev.* **26**, 153 (1981).
9. M. X. Zhang and P. M. Kelly, *Scripta Mater.* **48**, 647 (2003).
10. D. Duly, J. P. Simon, and Y. Brechet, *Scripta Metall. Mater.* **29**, 1593 (1993).
11. D. Duly, M. C. Cheynet, and Y. Brechet, *Acta Metall. Mater.* **42**, 3843 (1994).
12. A. Srinivasan, U. T. S. Pillai, and B. C. Pai, *Mat. Sci. Eng. A* **452-453**, 87 (2007).
13. B. A. Esgandari, H. Mehjoo, B. Nami, and S. M. Miresmaelil, *Mat. Sci. Eng. A* **528**, 5018 (2011).
14. I. C. Jung, W. T. Kim, and D. H. Kim, *Met. Mater. Int.* **20**, 99 (2014).
15. D. H. Kang, S. S. Park, N. J. Kim, *Mat. Sci. Eng. A* **413-414**, 555 (2005).
16. K. N. Braszczynska-Malik, *J. Alloy. Compd.* **477**, 870 (2009).
17. D. Duly, J. P. Simon, and Y. Brechet, *Acta Metall. Mater.* **43**, 101 (1995).
18. C. J. Bettles, *Mat. Sci. Eng. A* **348**, 280 (2003).
19. F. Findik, *J. Mater. Sci. Lett.* **17**, 79 (1998).